

RESEARCH PAPER

Preparation of CuO/PVA Nanocomposite Thin Films for Gamma Ray Attenuation via PLA Method

Kater Alnada Faris Husham¹, Huda M. Khدير², Noor M. Saadoon^{3*}, Ali M. Ahmed⁴

¹ Department of Chemical Engineering University of technology, Baghdad, Iraq

² Constration and project department, University of Technology, Baghdad, Iraq

³ Centre of nanotechnology and advanced material, University of Technology, Baghdad, Iraq

⁴ College of medicine , Mustansiriyah university ,Baghdad , Iraq

ARTICLE INFO

Article History:

Received 11 April 2024

Accepted 23 June 2024

Published 01 July 2024

Keywords:

CuO

Nanocomposite

Pulse Laser ablation

PVA

ABSTRACT

The laser ablation (PLA) method was used with different laser pulses to make copper oxide/polyvinyl alcohol (CuO/PVA) nanocomposite thin films. The effect of laser pulses on the optical, structural, morofigical, and roughness properties was investigated. X-ray diffraction (XRD) results confirmed the formation of CuO nanoparticles (NPs) after ablation of the target surface with a pulsed laser beam with high crystallinity and purity. The direction of crystal growth was in the (002) plane.

How to cite this article

Faris Husham K. A., Khدير H. M., Saadoon N. M., Ahmed A. M. Preparation of CuO/PVA Nanocomposite Thin Films for Gamma Ray Attenuation via PLA Method. J Nanostruct, 2024; 14(3):712-722. DOI:10.22052/JNS.2024.03.002

INTRODUCTION

One important technique for synthesizing nanoparticles with regulated size and geometry is pulsed laser ablation, or PLA. Shortly after the pulsed ruby laser was created in the 1960s [1], pulsed laser ablation was initially developed. Many researchers have since researched laser ablation in a diluted gas or vacuum. Multiple thin films can be produced by adjusting factors including laser wavelength, fluency, and pulse duration, as well as target materials and background gases. These comprise metals, semiconductors, oxides, and various ceramics that are high temperature superconductors [2] and diamond-like carbon [3]. Compared to silica-based optical materials,

polymer materials are easier to process, less expensive, and can be produced in large quantities [1]. By adding an opportunity dopant, a polymer's characteristics can be significantly enhanced and controlled [2]. The optical absorption of some metallic salts including Polyvinyl Alcohol (PVA) varies significantly, and the optical characteristics of doped polymers are highly reliant on the electrolytes' internal electrical arrangement. Understanding and managing the electrical mechanisms involved in the process is essential to producing materials with enhanced optical properties[3].The chemical formula of polyvinyl alcohol (PVA) is (C₂H₄O)_x, and its density ranges from 1.19 to 1.31 g/cm³. The melting point of PVA

* Corresponding Author Email: mae.visit.04@uotechnology.edu.iq



is 230°C. Because it can undergo pyrolysis at high temperatures, it decomposes quickly over 200°C [4]. PVA is typically modified and enhanced by the addition of various additives, including polymers, salts, nanocomposites, and ions [5]. The behavior of polymers and, more generally, composite materials with unique properties that differ from those of the matrix and filler may be demonstrated [6]. Numerous researchers examined the (PVA) films made by a casting procedure and filled with different mass fractions of FeCl₃. There was clarification on the structural, electrical, and magnetic properties. Certain IR absorption peaks' filling level (FL) dependence was connected with the physical parameter that was obtained to describe the other characteristics. [8].

MATERIALS AND METHODS

Materials

PVA polymer (C₂H₄O) forms Zhuzhou Chemical Company with purity of 99%. A high-purity copper (Cu) target form sigma aldrich company. Distilled water (DW) was used throughout the work.

PLA method

An Nd:YAG laser equipped with a lens with a

focal distance of 8 cm, pulse energy of 250 mJ, a pulse repetition frequency of 6 Hz, a duration of about 7 ns, and a wavelength of 532 nm was used to fabricate Cu-PVA polymer NPs as nanocomposites. A plate of high-purity CuO metal was used as the source of the NPs. 10 ml of a solution of PVA polymer dissolved in DW (at a concentration of 1 g of PVA per 10 ml of deionized water) was placed in a baker. The polymer solution and nanoparticles were then deposited on high-purity glass substrates at a temperature of 40°C. The thin film of the nanocomposite is kept in a closed vacuum to prevent contamination with impurities before testing.

Characterization

The powder X-ray diffraction (XRD; PANALYTICAL X PERT PRO-USA) study of the specimens' crystalline structure was conducted using a CuK α radiation source ($\lambda=1.5406 \text{ \AA}$) and an angle range of 20-80° (2 θ). A field emission scanning electron microscope (FESEM-DES; ZEISS SIGMA VP-GERMANY) was used to examine the morphology of CuO/PVA nanocomposite thin films. Xenon lamp spectrophotometers (Split-beam Optics, Dual detectors, Japanese built) were used to analyze

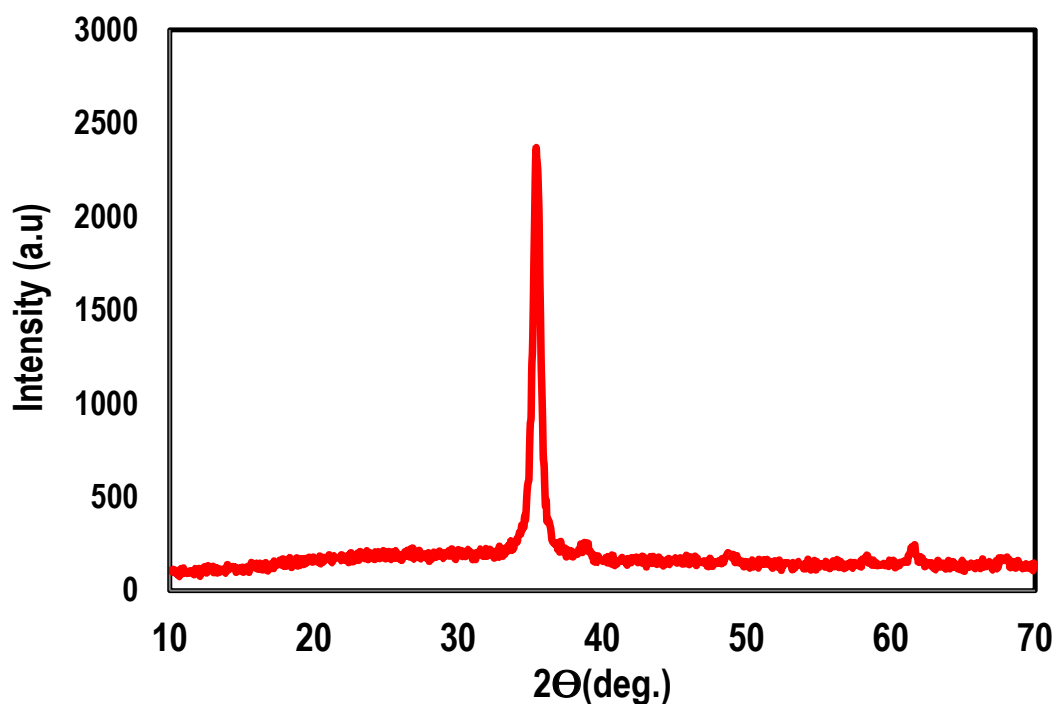


Fig. 1. XRD pattern of CuO nanoparticles

absorption spectra.

RESULTS AND DISCUSSION

The Structural Properties

X-Ray analysis (XRD) Results of CuO and Cu/PVA Nanoparticle

Fig. 1 Demonstrate the XRD pattern of the chemical reaction and laser ablation methods used to synthesize CuO nanoparticles. Using the techniques of pulse laser ablation and chemical reaction with solutions of ethylene glycol and water, preparation samples were placed on glass substrates. The structural analysis of synthesized materials was conducted using X-ray diffraction. The crystallinity is defined as the peaks sharp

of XRD while the broad peaks show the nature amorphous of the sample. When comparing the XRD pattern of CuO synthesized by laser ablation to CuO synthesized by chemical reaction, the former exhibits an amorphous nature with no prominent sharp peak following modification with a concentration of copper.

Scanning Electron Microscopes (SEM) and EDX Analysis of CuO Nanoparticle NPs

Scanning Electron Microscopy (SEM) was used to analyses the morphology of pure PVA, un-irradiated CuO nanocomposites, and irradiated Cu/PVA nanocomposites, as shown in Fig. 2. It was noted that the network structure of pure PVA is

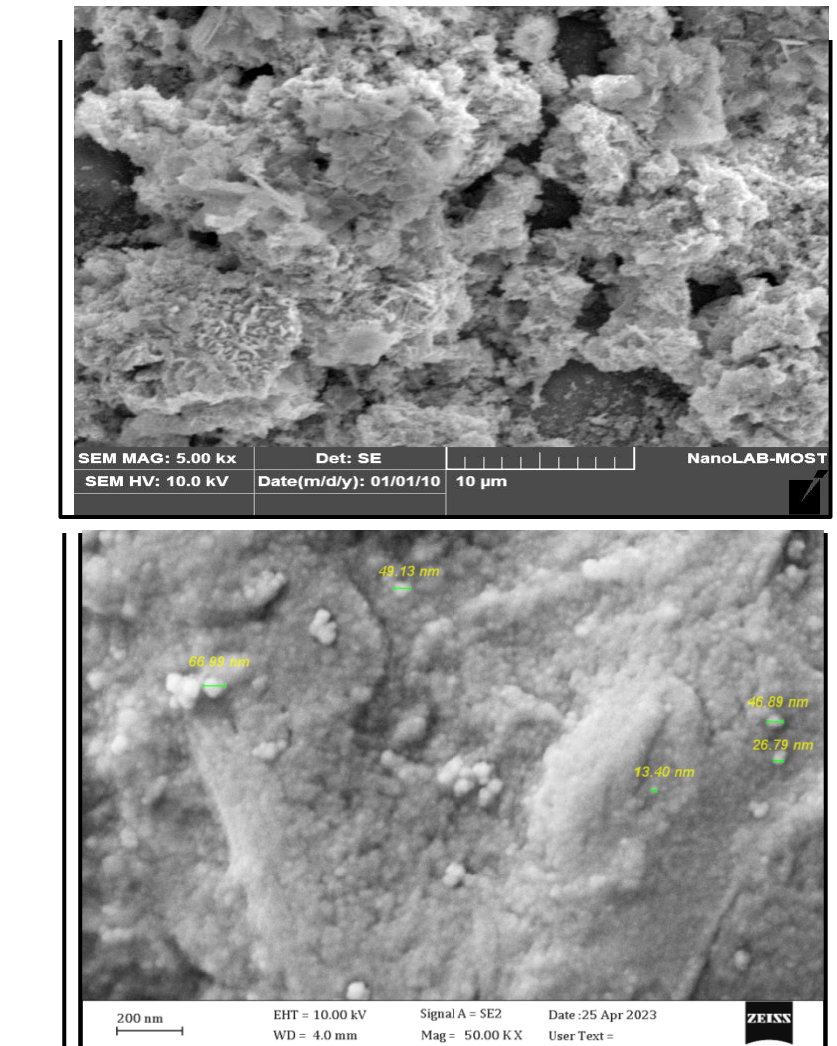


Fig. 2. SEM image of PVA,CuO thin film deposited on glass substrate prepared using pulse laser ablation method

soft. Cu nanoparticles were uniformly dispersed across the PVA film and had almost spherical forms. The images SEM of CuO and CuO thin film shown in Fig. 2 which prepared by substrate glass used the methods of PLA and chemical with athelen and water solution at energy pulsed (500 MJ), respectively. The elemental analysis using Energy Dispersive X-ray Spectroscopy verified the presence of Cu (EDX).

EDX analytical of CuO Nanoparticle

The EDX analysis, as shown in Fig. 3, demonstrated that the powder utilized as a support material during the shielding manufacturing process contained O and Cu elements. The EDX examination, shown in Fig. 3, confirmed that the electrochemically produced film included the components Cu and O. The type of salt employed in the experiment and PLA procedures on glass substrates with water and alcohol (ethylene) solvents caused other elements to arise in this process.

Optical characterization of CuO Nanoparticle NPs

Fig. 4 depicts the transmutation curve of CuO NPs produced by pulse laser ablation and electrochemical techniques utilizing laser energy of (500mj). Since an increase in laser energy causes a rearrangement of the surface of produced NPs and increases the transparency of films, it is obvious that the absorption decreases with

increasing laser energy for all prepared samples.

Fourier transform infrared (FT-IR)

The FT-IR spectra of PVA films implanted by CuO NPs at various laser energy (250, 500, 750, and 1000 pulsed number) are shown in Fig. 5. At 3305 cm^{-1} , the O-H stretching vibration for PVA has been removed. The C-H group's stretching symmetric vibrations are displayed at 2923 cm^{-1} . The stretching asymmetric vibrations of the C-H group have been seen at 2852 cm^{-1} . The vibrational band at 1725 cm^{-1} was ascribed to the C=C stretching vibration, at 1651 cm^{-1} the O-H bending vibration was eliminated, and at 1431 cm^{-1} the C-H group bending vibration was observed. The vibration wiggling of the C-H group was seen at 1375 cm^{-1} . The acetate remnants were observed to exhibit C-H wagging at 1242 cm^{-1} whereas the C-O stretching vibrations were detected at 1087 cm^{-1} and 1023 cm^{-1} . The shuffling The O-H group stretching vibration for PVP was recorded at 3405 cm^{-1} . At 1427 cm^{-1} and 1373 cm^{-1} , there are two bands for the C-H bending vibrations. At 1278 cm^{-1} , the C-N bending vibration was noted. At 1220 cm^{-1} and 1012 cm^{-1} , CH₂ bands vibrational were observed to shake and twist. (N-C=O) bending vibrations are ascribed to the band at 564 cm^{-1} . At energy pulsed laser (250 mj) of the Cu/PVA film blend, found shift in O-H vibration stretching, new bands at $1740, 1490, \text{ and } 1250\text{ cm}^{-1}$, corresponding to the vibrations of C=O stretching, C-H bending,

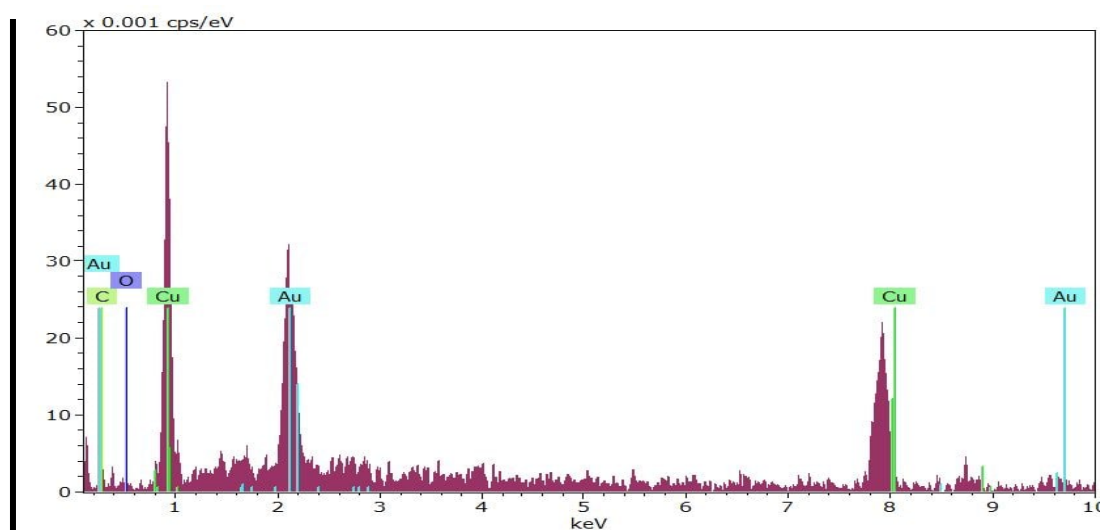


Fig. 3. EDX analysis of CuO NPs prepared by electrochemical method on glass

and C-O-C stretching, were also seen. The bands at 1644 cm^{-1} shifted as well, and all of the bands' intensities decreased [12].

The peaks from DMF that are linked to the stretching vibrations of C=O, C-N, and C-H are located at 1659 , 1415 , and 1044 cm^{-1} , respectively. The carbonyl C=O bond's bond order decreases

while the carbon-nitrogen bond's bond order increases as a result of the two potential resonance configurations of an amide. A wide band can be seen in the spectrum between 3100 and 3600 cm^{-1} because of the hydrogen bonds that exist between the molecules of water. The O-H bond is influenced by the stretching frequency of 3344 cm^{-1} [13]. This

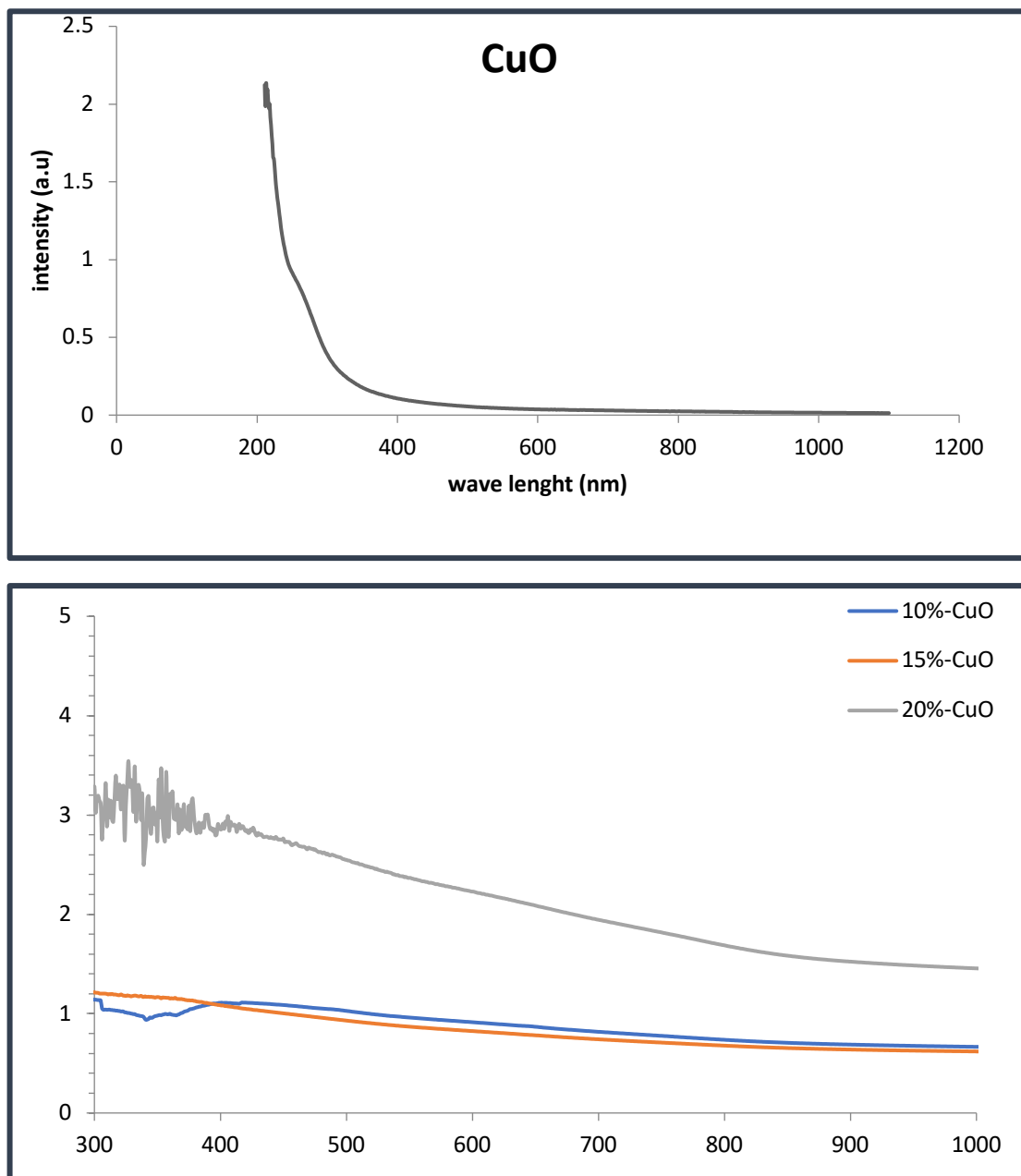


Fig. 4. The Transmission curve as a function of wavelength of CuO prepared using chemical method with water and athylen solution

indicates that the presence of ethyl or water in the system indicates the existence of the alkyl group.

surface morphology of NPs prepared in different energy

Figs. 7 a-d show the shape of the three-dimensional surface of NPs created at different energies. Energy has a significant impact on

the surface morphologies of CuO samples, as demonstrated by the extensive AFM investigation of these materials. Fig. 6a clearly shows that the films' grain sizes are growing as energy levels rise. Examination of the AFM images revealed that thin film columnar structures are apparent and the grain sizes are tiny at the start of growth which was vertical small and dense. The tiny

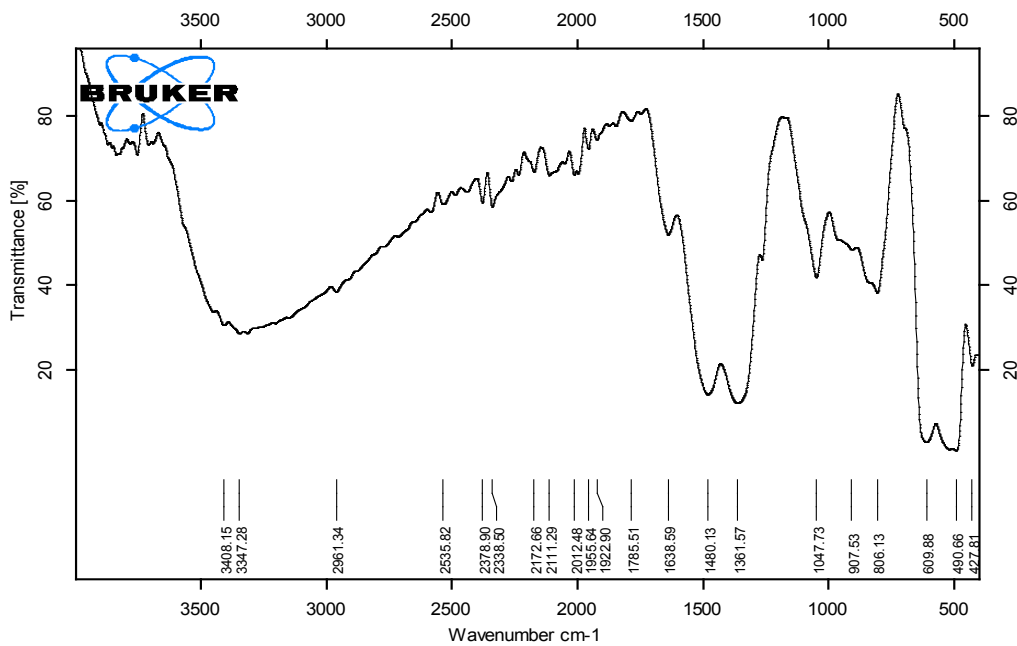


Fig. 5. FTIR spectrum for CuO nanoparticles.

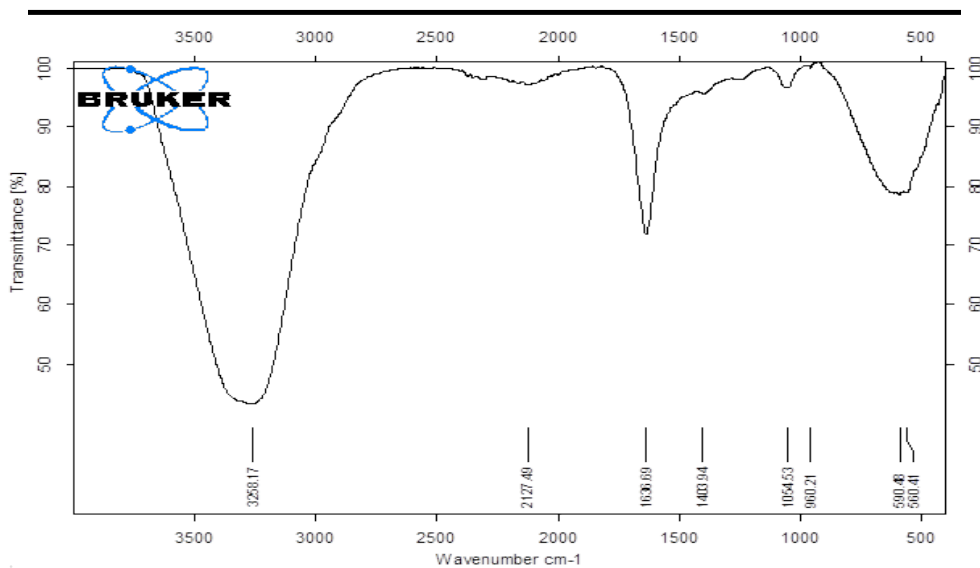
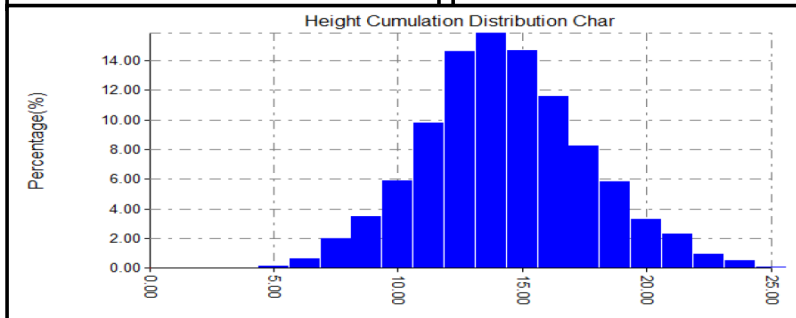
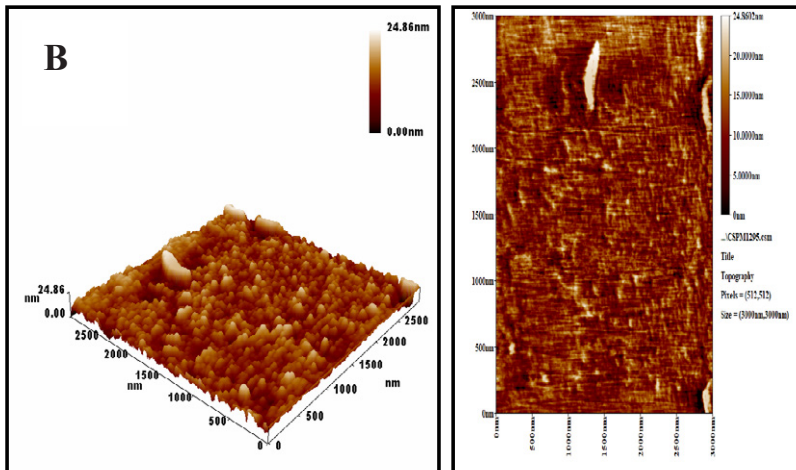
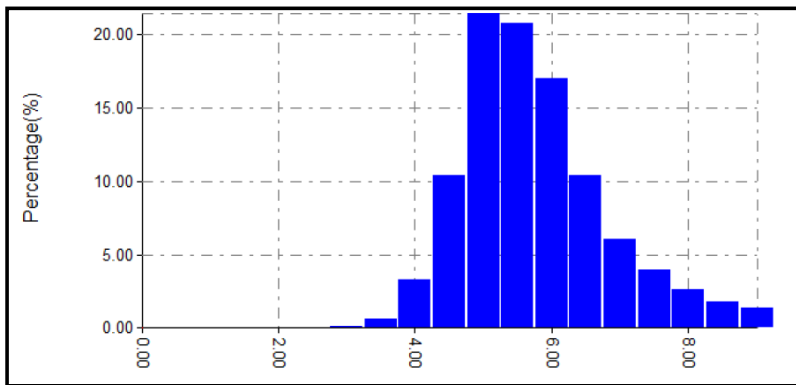
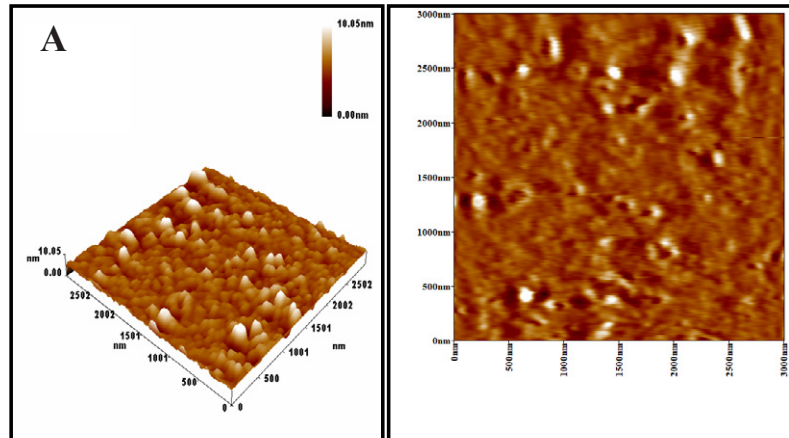


Fig. 6. FTIR spectrum for CuO nanoparticles synthesis by LA.



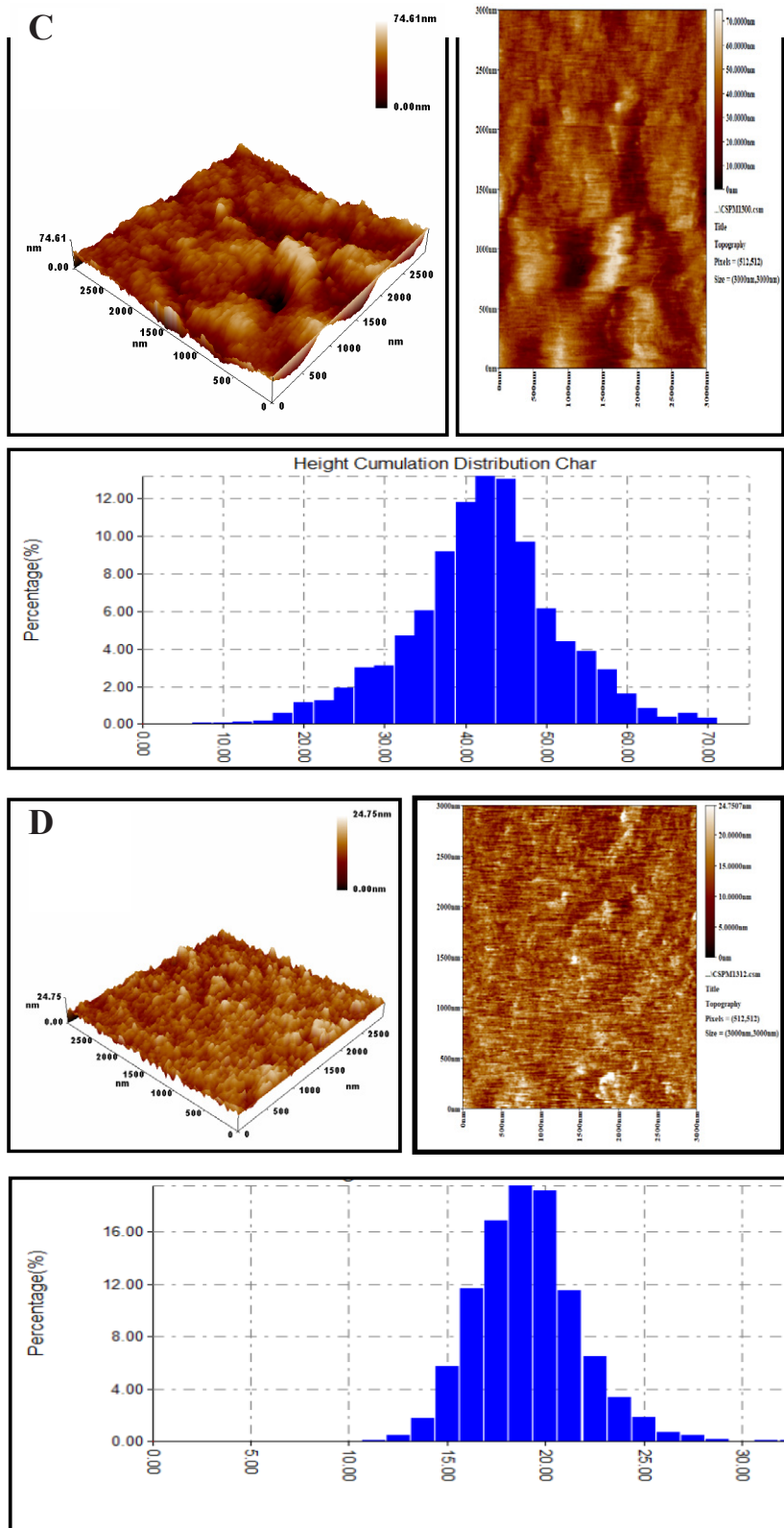


Fig. 7. AFM images of Cu/PVA NPs at pulses energy (a) 250 m, (b) 500, (c) 750, (d) 1000 pulsed.

grains gathered to become the largest grains when energy levels rose. (Figs. 6b, 6c). When the energy was 500mj and the pulse number was increased to 1000 pulsed, the grains will become much bigger and may be caused clusters, these clusters are combined and produced bigger grains and also the roughness of surface of Cu films was studied by AFM. Fig. 6b shows how increasing the film energy from 250 to 1000 pulses causes the surface roughness to increase from 0.10 to 2.91 nm, which in turn causes the grain size to expand from 20 to 35 nm. The roughness of a film's surface can be significantly influenced by the surface morphology of the glass substrate [14-15].

The Table 1 shows the effect of laser pulsed energy on the roughness of the surface also the effect on the crystalline size.

Fig. 7 displays the roughness (RMS) values of CuO NPs together with AFM photos. As the annealing temperature rose, the grain size increased as well. This can be explained by the thermal energy that annealing provides, which is used by active species to fill in the micro-voids or flaws between columnar formations. As a result, roughness increased as particle size increased [16]. This phenomenon confirms the findings of the earlier investigation regarding the connection between grain growth and roughness.

Shielding parameters

Linear attenuation coefficient μ_l

Fig. 8 displays the linear attenuation coefficient of the Cu/PVA shield at different energies. It is evident that as the laser emerges more, the values

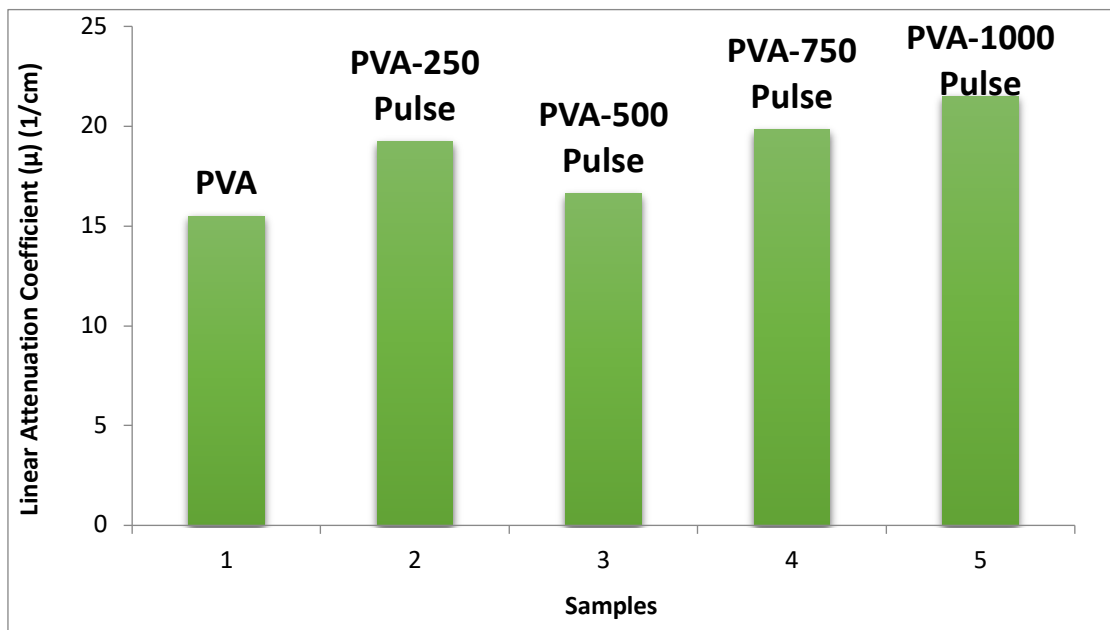


Fig. 8. displays the Cu/PVA shield's linear attenuation coefficient at various energies

Table 1. The laser energy and RAS of the CuO NPs

Laser energy(500mj) while pulse number	SA	RMS	Crystalline size (D)nm
250	0.731	1.02	25
500	1.34	1.73	33
750	7.52	9.87	42
1000	2.29	2.91	38

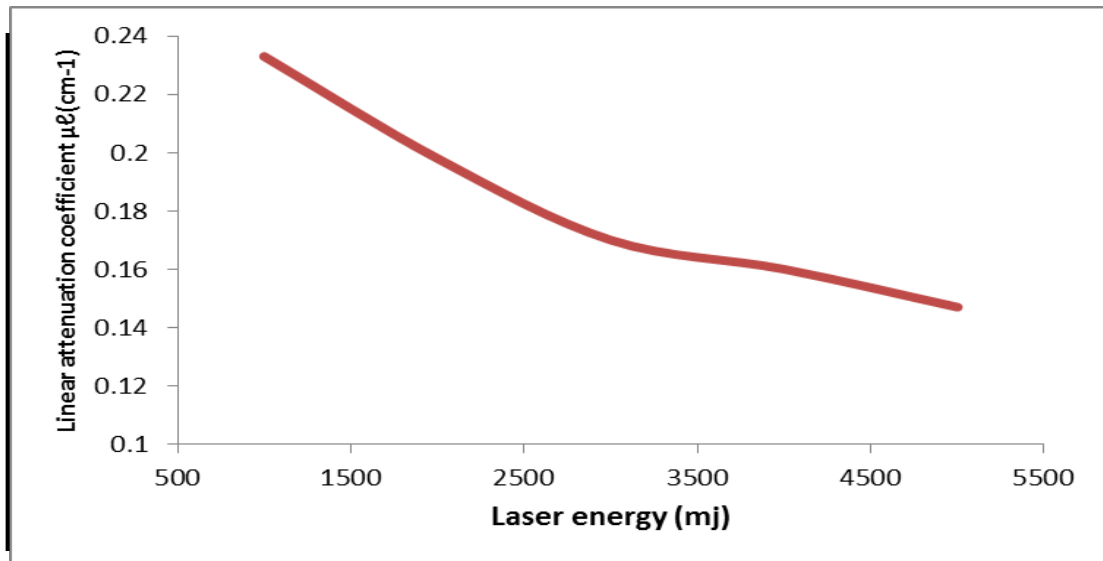


Fig. 9. Relationship between the linear attenuation coefficient and different laser energy (1000, 2000, 3000, 400 and 5000) mj.

Table 2. The laser energy and seling parameters of the CuO-pva nanocomposite

SAMPLE	I	IO	X(nm)	X(cm)	U	HVL	TVL
LASER ENERGY							
1000	500	370	172.5	0.00001725	-17455.4	-3.971E-05	-0.00013191
2000	510	370	185.2	0.00001852	-17327.6	-4.0002E-05	-0.00013289
3000	495	370	179.5	0.00001795	-16214.7	-4.2748E-05	-0.00014201
4000	505	370	218.4	0.00002184	-14242.5	-4.8668E-05	-0.00016167
5000	440	370	218.4	0.00002184	-7933.69	-8.7368E-05	-0.00029023

of the linear attenuation coefficient increase. [17] Additionally, Table 2 shows that the enhanced distribution of laser energy material will lead to an increase in absorption processes, which raises the shield density, gamma ray attenuation, and the linear attenuation coefficient as a result. [18] One could argue that PVA is ineffective as a gamma radiation shield on its own. Fig. 9 shows the relationship between various laser energy and linear attenuation coefficient for different concentration of the material composite of the reinforcement material.

CONCLUSION

Copper Oxide thin films Prepared successfully, using PLA method and chemical method deposited on a glass substrate by using spin coating

technique. The XRD pattern of CuO synthezied by laser ablation method indicates that the nature is amorphous without a sharp peak prominent after being modified with a concentration of copper. Narrow FWHM, low strain, and small crystalline size have been observed. The diffraction planes for physical and chemical method. The surface morphology of CuO thin film deposition on the glass substrates at different synthesis methode are measured by using Atomic force microscopy (AFM) which is observed the average Roughness of the CuO thin films that depended on the crystallization degree. The Cu/PVA material and its application in shielding application very promising in nanotechnology, which has an active role in the behavior of factors affecting the manufacture of nuclear shields.



CONFLICT OF INTEREST

The authors declare that there is no conflict of interests regarding the publication of this manuscript.

REFERENCES

1. Vashistha P, Gaur SS, Tripathi KN. Characterization of ammonium dichromate doped PVA films based waveguides. *QEE*. 2007;39(9):717-721.
2. Podgrabinski T, Švorčík V, Macková A, Hnatowicz V, Sajdl P. Dielectric properties of doped polystyrene and polymethylmethacrylate. *Journal of Materials Science: Materials in Electronics*. 2006;17(11):871-875.
3. Abdullah OG. Optical Properties of PVA: CdCl₂·H₂O Polymer Electrolytes. *IOSR Journal of Applied Physics*. 2013;4(3):52-57.
4. Ghanipour M, Dorrani D. Effect of Ag-Nanoparticles Doped in Polyvinyl Alcohol on the Structural and Optical Properties of PVA Films. *Journal of Nanomaterials*. 2013;2013:1-10.
5. Khalifa N, Souissi A, Attar I, Daoudi M, Yakoubi B, Chtourou R. Uncommon photoluminescence behavior of Fe³⁺ doped polyvinyl alcohol films. *Optics & Laser Technology*. 2013;54:335-338.
6. Shaheen A, Taqmeem H, Aamir S, Qamar ul I. The Feasibility of Reactive Dye in PVA Films as High Dosimeter. *Journal of Basic & Applied Sciences*. 2021;9:420-423.
7. Vijaya Kumar G, Chandramani R. Doping and Irradiation Dependence of Electrical Conductivity of Fe³⁺ and Ni²⁺-Doped Polyvinyl Alcohol Films. *Acta Physica Polonica A*. 2010;117(6):917-920.
8. Tawansi A, El-Khodary A, Abdelnaby MM. A study of the physical properties of FeCl₃ filled PVA. *CAP*. 2005;5(6):572-578.
9. Meena K, Lawrance R. News document analysis by using a proficient algorithm. *International Journal of Engineering Research and Applications*. 2017;07(06):07-13.
10. Thiele H. Kozelka, R. M.: *Elements of Statistical Inference*. Addison-Wesley Publishing Company, Inc. Reading, Massachusetts, London 1961. x + 150 S., 42 Abb., 4 Tabellen, 38 s. *Biom Z*. 1962;4(3):210-210.
11. Gokul B, Matheswaran P, Sathyamoorthy R. Influence of Annealing on Physical Properties of CdO Thin Films Prepared by SILAR Method. *Journal of Materials Science & Technology*. 2013;29(1):17-21.
12. Choppali U, Gorman BP. Structural and optical properties of nanocrystalline ZnO thin films synthesized by the citrate precursor route. *Journal of Luminescence*. 2008;128(10):1641-1648.
13. Lindström BO. *X-Ray Absorption Microanalysis. X-ray Optics and X-ray Microanalysis*: Elsevier; 1963. p. 13-22.
14. Gay P. A. J. C. Wilson. *Elements of X-ray Crystallography* Reading, Massachusetts Addison-Wesley 1970 ix+256 pp., 64 figs. Price \$14.75. MinM. 1971;38(293):114-114.
15. Dhanam M, Prabhu RR, Manoj PK. Investigations on chemical bath deposited cadmium selenide thin films. *Materials Chemistry and Physics*. 2008;107(2-3):289-296.
16. Dakhel AA. Structural and optical properties of evaporated Zn oxide, Ti oxide and Zn-Ti oxide films. *Appl Phys A*. 2003;77(5):677-682.
17. Krishnakumar V, Shanmugam G. Electrical and optical properties of pure and Pb²⁺ ion doped PVA-PEG polymer composite electrolyte films. *Ionics*. 2011;18(4):403-411.
18. Electrical Properties of poly Vinyl Alcohol (PVA) doped with Alizarin orange Azo dye thin films prepared by cast method. *University of Thi-Qar Journal of Science*. 2019.